Critical properties of the four-state commutative random permutation glassy Potts model in three and four dimensions

L. A. Fernández,[1,2] A. Maiorano,[2,3] E. Marinari,[4] V. Martin-Mayor,[1,2] D. Navarro,[5,6] D. Sciretti,[2,7] A. Tarancón,[2,7] and J. L. Velasco[2,7]

[1]*Departamento de Física Teórica I, Facultad de Físicas, Universidad de Complutense, 28040 Madrid, Spain*

[2]*Instituto de Biocomputación y Física de Sistemas Complejos (BIFI), 50009 Zaragoza, Spain*

[3]*Dipartimento di Fisica, Università di Ferrara, I-44100 Ferrara, Italy*

[4]*Dipartimento Fisica, INFN and INFM, Sapienza Università di Roma, 00185 Roma, Italy*

[5]*Instituto de Investigación en Ingeniería de Aragón (I3A), Universidad de Zaragoza, 50018 Zaragoza, Spain*

[6]*Departamento de Ingeniería Electrónica y Comunicaciones, Centro Politécnico Superior, Universidad de Zaragoza, 50018 Zaragoza, Spain*

[7]*Departamento de Física Teórica, Facultad de Ciencias, Universidad de Zaragoza, 50009 Zaragoza, Spain*

(Received 26 October 2007; revised manuscript received 26 February 2008; published 24 March 2008)

We investigate the critical properties of the four-state commutative random permutation glassy Potts model in three and four dimensions by means of Monte Carlo simulations and a finite-size scaling analysis. By using a field programmable gate array, we have been able to thermalize a large number of samples of systems with large volume. This has allowed us to observe a spin-glass ordered phase in $d=4$ and to study the critical properties of the transition. In $d=3$, our results are consistent with the presence of a Kosterlitz-Thouless transition, but also with different scenarios: transient effects due to a value of the lower critical dimension slightly below 3 could be very important.

DOI: 10.1103/PhysRevB.77.104432 PACS number(s): 75.10.Nr, 64.60.F−, 05.10.Ln

I. INTRODUCTION

In the last years, spin-glass models without spin-inversion symmetry[1–9] have received a large amount of attention: probably the main reason for this large effort is that these models are thought to describe structural glasses that in nature, as opposed to spin glasses, do not enjoy this symmetry. One of them, the ferro–Potts-glass (FPG) model,[2,3] is a very direct generalization of the Ising-Edwards-Anderson spin-glass model: the spins can take p different values, and two neighboring spins contribute to the total energy a factor $-J_{ij}$ if they are in the same state and a factor $+J_{ij}$ if they are in different states. The bonds J_{ij} are quenched random variables that can be distributed, for example, under a Gaussian or under a bimodal distribution. In the FPG model, as we will discuss better in the following, the missing spin-inversion symmetry has the collateral effect of allowing the existence of a ferromagnetic phase at low values of the temperature (this is why we define it as a ferro–Potts-glass model): because of this possible contamination, the analysis of the glassy critical points of the model can potentially become very complex and even lead to misleading conclusions. In fact, as we will discuss below, progress can be expected from the consideration of more refined models, where gauge symmetry forbids the ferromagnetic phase.

The FPG model is a candidate for describing orientational glasses: a p-state spin models a quadrupole moment which can be directed in p (discrete) directions.[10] However, its main interest maybe originates from some of the properties of its infinite-range version: for $p>4$, for example, the mean-field FPG undergoes a glass transition[4] where the order parameter is discontinuous.[11] A number of different lattice models,[1–3,5–8,12] in other words, can be analyzed to clarify the finite-range behavior of systems showing the equilibrium properties typical of glasses: it is also important to remember that a number of important connections have been found[13,14] between the mean-field dynamical equations of the model and the mode-coupling theory of the structural glass transition,[15,16] which describes the evolution of the density correlations in a supercooled liquid above the dynamical transition temperature.

Even if the mean-field results are an important starting point, in a next step, since real systems have short-range interactions, it is important to study finite-dimensional systems. A great part of the mainly numerical effort has been focused on the $p=3$ model in $d=3$ to model a realistic quadrupolar glass.[17] The first numerical studies[18–25] found that the lower critical dimension d_l is close to 3. In a numerical study with a zero-temperature scaling approach, Banavar and Cieplak[18] suggested that the FPG with Gaussian couplings has a d_l slightly greater than 3, while the FPG with bimodal couplings has a d_l slightly below 3 (but such a measurement had large intrinsic errors). A few months later Monte Carlo simulations[20,21] hinted that the transition seems to take place at a temperature compatible with $T_c=0$ for both families of couplings, which suggested indeed that $d_l=3$. Further simulations in the bimodal[22] and Gaussian[23] models were consistent with these results, although one could not exclude the possibility of T_c being small but larger than zero. A later study based on a high-temperature expansion[24,25] did not allow a final conclusion to be reached. Only recently have we started to have clearer evidence about the situation: a large-scale numerical study, based on a finite-size scaling analysis of the correlation length,[26] gives what looks like reliable evidence of a transition to a glass phase at finite T_c, making in this way a strong case for d_l being slightly below 3 for the three-state FPG model.

Another interesting model that has been studied in detail is the $p=10$ model in $d=3$, because of the intrinsic interest of

the limit of a large number of states. Old[27,28] and recent[26] numerical simulations seem to suggest that there is no spin-glass transition at finite temperature (but all the warnings about the dangers of ferromagnetic effects at low T in this model stay in effect). This finding is in marked contrast with the predictions of mean-field theory, which indeed undergoes two transitions[13,14]: new models could be useful to understand better the connections among the mean-field and finite-dimensional picture, and, for example, Potts-glass models with medium-range interactions[27,28] could be relevant for this effect.

It has also been argued[29] (although some controversy exists[28]) that the choice of the coupling distribution might be relevant in removing the phase transition on the $p=10$ model. The deficiency of the FPG model that we have discussed before is the designated culprit: the lack of spin inversion symmetry (which in Ising spin glasses is connected to a gauge symmetry that forbids a spontaneous magnetization[30]) allows ferromagnetic ordering at low temperatures.[2,3] A partial relief to this problem can be obtained by using a distribution of couplings nonsymmetric around zero,[26,27] but this choice does not recover the lost (important) gauge invariance.

A different (and natural) definition of a frustrated Potts model containing quenched disorder, the random-permutation Potts-glass (RPPG) model, was introduced a few years ago.[6] The key point of the RPPG model [and of a similar model where only a set of possible couplings is allowed, the commutative random-permutation Potts glass (CRPPG) model, where an additional symmetry is very useful to help checking thermalization; see Sec. II A] is that it retains the gauge invariance which prevents Ising spin glasses from entering ferromagnetic ordering at low temperature. The same paper[6] analyzed numerically the $p=4$, four-dimensional model (in both in the RPPG and CRPPG versions) on lattices of volume $V=4^4$ and $V=5^4$. The two models were found to exhibit the same critical behavior, with a glassy phase characterized by a divergence of the overlap susceptibility. A preliminary value of γ was estimated from that divergence, and the critical temperature was obtained from the analysis of the Binder parameter: the critical behavior was found to be reached under a discontinuity, which was related to the one observed in the random-energy model.[12] It is also interesting to note that Carlucci[31] has discussed the relation connecting the (C)RPPG and the chiral-Potts model, the latter introduced by Nishimori and Stephen,[5] which in mean field shows the same type of transition for $p>4$.[4,31] The authors of Ref. 6 also present a dynamical study of their models, and they observe clear aging effects.

In this work we investigate, by means of Monte Carlo simulation and finite-size scaling analysis, the critical properties of the three- and four-dimensional $p=4$ CRPPG model. In $d=3$, the finite-size behavior makes it possible for the system to undergo a Kosterlitz-Thouless transition, although a d_l barely lower than 3 is surely compatible with the significance of our numerical data. In $d=4$, we confirm the existence of the spin-glass transition reported in Ref. 6, but the use of a field programmable gate array (FPGA) computer (see the Appendix and Ref. 32) allows us to obtain more accurate estimates of the critical exponents, universal dimensionless quantities, and nonuniversal critical couplings of the model.

The remainder of this work is organized as follows. In Sec. II A we define the model and comment on its symmetries. We describe the relevant observables in Sec. II B. Section III is devoted to a discussion of the numerical methods: the details of the simulations are described in Sec. III A and the finite-size scaling method in Sec. III B. Further details about the computation are given in Sec. III C, while the problem of thermalization is addressed in Sec. III D. The results for the $d=3$ model are discussed in Sec. IV, and those for $d=4$ are discussed in Sec. V. We present our conclusions in Sec. VI. In the Appendix we give details about the FPGA and about how they have actually been used.

II. MODEL

A. Model and symmetries

We consider a system of spins $\{\sigma_i\}$ defined on a $d=3$ (and $d=4$) dimensional simple cubic lattice of linear size L (volume $V=L^d$) and periodic boundary conditions. The Hamiltonian is

$$H \equiv -\sum_{\langle i,j \rangle} \delta_{\sigma_i,\Pi_{ij}(\sigma_j)}, \tag{1}$$

where the sum runs over all pairs of nearest-neighboring sites. The spins can take the values $\{0,1,2,3\}$, and Π_{ij} are quenched permutations of $\{0,1,2,3\}$, defined on the links of the lattice.[6,33] We define our quenched couplings (to implement the commutative model of Ref. 6) by extracting random permutations of (0,1,2,3) that commute with our "reference permutation" $R=(0,1,2,3)\rightarrow(2,3,0,1)$. Only links from i to j such that $\sigma_i=\Pi_{ij}(\sigma_j)$ give a nonzero contribution to the energy. The RPPG and CRPPG models are deeply connected[31] to the chiral-Potts model analyzed by Nishimori and Stephen.[5]

The symmetry with respect to the reference permutation R helps in defining an order parameter q governed by a probability distribution symmetric under $q\rightarrow -q$ (this turns out to be crucial for checking that the system has reached thermal equilibrium[6]). We define two copies of the system (two real replicas) $\{\sigma_i^{(1)}\},\{\sigma_i^{(2)}\}$, and we allow them to evolve independently at the same temperature and the same realization of quenched random couplings Π_{ij}. The *modified* overlap between the two replicas at site i is defined as

$$q_i = \begin{cases} 1 & \text{if } \sigma_i^{(1)} = \sigma_i^{(2)}, \\ -1 & \text{if } \sigma_i^{(1)} \neq \sigma_i^{(2)} \quad \text{and} \quad \sigma_i^{(1)} = (\sigma_i^{(2)}+2) \bmod 2, \\ 0 & \text{elsewhere.} \end{cases} \tag{2}$$

B. Observables

The main quantities that we will consider here are defined in terms of the Fourier transform of q_i:

$$\hat{q}(\vec{k}) = \frac{1}{V}\sum_i e^{-i\vec{k}\cdot\vec{r}_i} q_i. \tag{3}$$

The momentum-space propagator is defined from the relation

$$G(\vec{k}) = V\overline{\langle \hat{q}(\vec{k})^2 \rangle}. \tag{4}$$

In the thermodynamic limit and at the critical point, the propagator is expected to have poles at $\vec{k}=\vec{0}$:

$$G(\vec{k}) \approx \frac{Z\xi^{-\eta}}{(\vec{k})^2 + \xi^{-2}}, \tag{5}$$

where the correlation length ξ diverges at the critical point and $\xi\|\vec{k}\| \ll 1$. We also define the nonconnected susceptibility

$$\chi = G(\vec{0}). \tag{6}$$

On a finite lattice an extremely useful definition of the correlation length can be obtained from the discrete derivative of $G(\vec{k})$. Using $\vec{k}=(2\pi/L)\vec{e}_\mu$, where $\vec{e}_\mu$ belongs to the canonical Cartesian basis, one obtains[34,35]

$$\xi = \left(\frac{G(\vec{0})/G(\vec{k}) - 1}{4\,\sin^2(\pi/L)} \right)^{1/2}. \tag{7}$$

We also compute and analyze the cumulant

$$U_4 \equiv \frac{\overline{\langle \hat{q}(\vec{0})^4 \rangle}}{\overline{\langle \hat{q}(\vec{0})^2 \rangle^2}}. \tag{8}$$

We define the energy as

$$E = \frac{4}{3Vd}\langle H \rangle - \frac{1}{3}, \tag{9}$$

so that it lies in the $[0,1]$ interval. When we need to estimate the derivative with respect to β of an observable O, we estimate it by measuring the connected correlation function $\langle OH \rangle_c$. Bias-corrected[36] reweighting techniques[35,37,38] allow us to use the numerical data taken at temperature T to compute expectation values at nearby temperature values T' and to get in this way estimates that cover all the relevant parts of the critical region.

III. NUMERICAL METHODS

A. Simulations

In the $d=3$ model we have analyzed lattices of linear sizes $L=6$, 8, 10, and 16. The critical behavior of the model (see Sec. IV) has suggested to simulate a wide range of values of β, ranging from 1.5 to 2.7. We have analyzed between 200 and 400 different samples of the smaller systems and around 1000 samples for $L=16$.

In $d=4$, we have analyzed lattices of linear sizes $L=8$, 12, and 16, with β ranging from 1.385 to 1.5. The main computer effort has been accomplished around $\beta=1.405$ and $\beta=1.41$, close to the critical point. At these temperatures, we have simulated 1000 samples for $L=8$ and 2000 samples for $L>8$. For the other β values we have simulated between 200 and 400 samples. We have also analyzed 50 samples of the system deep into the low-temperature region, at $\beta=1.5$.

B. Finite-size scaling

We give here a few details about the finite-size scaling approach that we have used for our analysis. When using the *quotient method*[35,39,40] one compares the mean value of an observable O, in two systems of sizes L_1 and L_2, using the value β where the correlation length in units of the lattice sizes coincides for both systems. If, for the infinite-volume system, $\langle O \rangle(\beta) \propto |\beta - \beta_c|^{-x_O}$, the basic equation of the quotient method is

$$Q_O^{L_1,L_2} \equiv \left. \frac{\overline{\langle O(\beta,L_2)\rangle}}{\overline{\langle O(\beta,L_1)\rangle}} \right|_{\xi(L_2,\beta)/\xi(L_1,\beta)=L_2/L_1} = \left(\frac{L_2}{L_1}\right)^{x_O/\nu} (1 + A_O L_1^{-\omega} + \cdots), \tag{10}$$

where the ellipsis stands for higher-order scaling corrections, ν is the correlation length critical exponent, ω is the (universal) first irrelevant critical exponent, and A_O is a nonuniversal amplitude.

Just below the lower critical dimension, at a distance ε, the critical exponent $1/\nu$ is expected to be of order ε. This means that, for a limited range of lattice sizes, the slope of the ξ/L curves at T_c grows very slowly (almost logarithmically) with L. This could make it difficult for a numerical study where one looks for a crossing of the ξ/L curves, since the curves for the different lattice sizes would be basically parallel in the critical region. In other words, distinguishing a *merging* of the ξ/L curves from a *crossing* becomes very hard. If one works precisely at the lower critical dimension (i.e., $\varepsilon=0$), one may expect that one of two mutually excluding scenarios is realized. If $T_c=0$, the curves for ξ/L would not join (if plotted versus $1/T$, the curves for lattices of size L and $2L$ should displace uniformly by an L-independent amount). On the other hand, if $T_c>0$, one would have a Kosterlitz-Thouless picture, where the curves for ξ/L merge for all $T<T_c$. It is clear that distinguishing a Kosterlitz-Thouless scenario from $\varepsilon>0$ but very small is numerically challenging.

The most precise way of extracting the critical point β_c is to consider the crossing point of dimensionless quantities such as ξ/L and U_4. When comparing their values in two systems of size L_1 and L_2, one finds that they take a common value at

$$\beta_c^{L_2,L_1} = \beta_c + B\frac{1-(L_2/L_1)^{-\omega}}{(L_2/L_1)^{1/\nu}-1} L_1^{-\omega-1/\nu} + \cdots. \tag{11}$$

The nonuniversal amplitude B depends on the dimensionless quantity that one considers.

C. Computational details

In order to compute equilibrium expectation values we update the spins with a sequential Metropolis algorithm, we bring them to equilibrium and during the equilibrium dynamics we measure the interesting physical quantities. Using our optimized FPGA-based processor, we have been able to run large-scale simulations: for example using strong thermalization tests, we can be sure that we have thermalized systems

TABLE I. For each lattice size of the $d=3$ model, we show the simulated temperatures, number of samples, number of EMCSs per sample, and EMCSs per measurement.

L	β	$N_{\text{samples}} \times 10^2$	EMCS $\times 10^6$	EMCS/meas.
6	1.6	2	4	40
6	2.0	2	4	40
6	2.4	4	4	40
8	1.6	2	4	40
8	1.8	2	8	40
8	2.0	4	8	40
8	2.4	4	4	40
10	1.5	2	4	40
10	1.8	2	12	40
10	2.0	2	12	40
10	2.2	4	12	40
10	2.4	4	24	40
16	1.8	10	60	5×10^5
16	2.0	10	60	5×10^5
16	2.2	10	60	5×10^5
16	2.4	9	600	2×10^6

of volume $V=16^3$ and $V=16^4$ at high β values, already deep in the broken phase. We define an *elementary Monte Carlo sweep* (EMCS) as V sequential trial updates of lattice spin (considered in lexicographic order). To produce the needed pseudorandom numbers we use the Parisi-Rapuano shift register method.[41]

The $d=3$ small lattices, from $L=6$ to 10, have been simulated at the cluster of the Instituto de Biocomputación y Física de Sistemas Complejos (BIFI). We have taken our measurements after every 40 EMCSs. The total simulation time for this set of lattices has been equivalent of 0.2 years of a Pentium IV processor running at 3.2 GHz. Our main effort in $d=3$ has concerned the large, $L=16$ lattice and has been simulated in a single FPGA (see Sec. VI for details). The total simulation time corresponds to almost 22 years of Pentium IV at 3.2 GHz. Table I shows the details of the computation.

In the $d=4$ model, lattices with $L=8$ and $L=12$ have been simulated at the BIFI Cluster. The total simulation time has been the equivalent to about 3 years of Pentium IV at 3.2 GHz. Again, the core of the simulation corresponds to lattice $L=16$, and has been computed with the FPGA. The total simulation time has been about 300 years-equivalent of Pentium IV. Measurements have been made every 5×10^5 EMCS. The details of the computation are shown in Table II.

D. Thermalization tests

This large computer effort has allowed us to thermalize in the broken phase lattices of volume including up to 65 536 spins (a large number). The thermalization issue is crucial in spin glasses, and we have checked it by several independent tests.

TABLE II. Same as Table I for $d=4$.

L	β	$N_{\text{samples}} \times 10^2$	EMCS $\times 10^6$	EMCS/meas.
8	1.41	10	4	40
8	1.44	10	4	40
8	1.5	10	4	40
12	1.41	20	6	40
16	1.385	2.8	60	5×10^5
16	1.395	8.5	60	5×10^5
16	1.405	10	60	5×10^5
16	1.41	2.5	200	5×10^5
16	1.44	4.8	500	5×10^5
16	1.5	0.5	1000	10^6

As a first tool we have used a logarithmic binning procedure. Let us say that during a Monte Carlo simulation we have collected estimates for an observable quantity O at all integer times t in the interval $[0,T)$. We divide these data in *bins* $I_n=[T/2^{n+1},T/2^n)$ for $n=0,1,2,3,\ldots$. The usual disorder average of O, $\overline{\langle O\rangle}$, is obtained (after assuming that all data are at equilibrium) by averaging all Monte Carlo data—i.e., the data over all bins. Information about thermalization can be obtained by averaging separately over samples the time series in the different bins. We get in this way the logarithmic running disorder averages $O_n \equiv \overline{\langle O\rangle}_n$. In the usual logarithmic data binning, if thermalization has been achieved, one expects that O_n becomes n independent for small n (the last bins). We show this quantity (shifted by O_0 for a better comparison with $\delta_n O$; see below) in the case of the nonconnected susceptibility as a function of the logarithmic binning level n in Fig. 1. The data correspond to the four-dimensional system of volume $V=16^4$ at two values of the temperature, one very close to the critical point and one in the low-temperature phase: the errors are drawn with a thin line.

An even better control of the convergence with time to the asymptotic result can be obtained by computing the difference of the thermal expectation value in bin n and the value

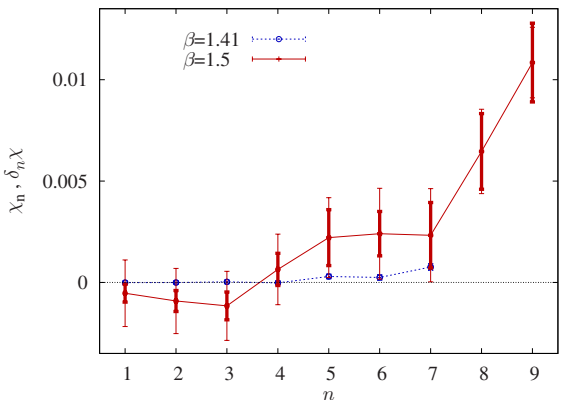

FIG. 1. (Color online) Logarithmic data binning analysis (see text) of the nonconnected susceptibility for the $d=4$ model, $L=16$, $\beta=1.41$, and $\beta=1.5$. Notice that the large time region appears on the left in the figure.

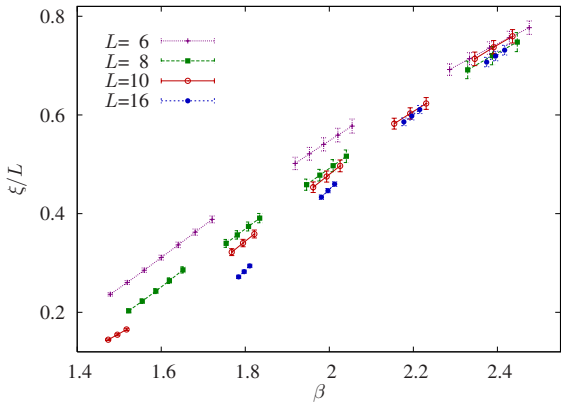

FIG. 2. (Color online) Correlation length in units of the linear size L as a function of β for $d=3$ systems of different volumes.

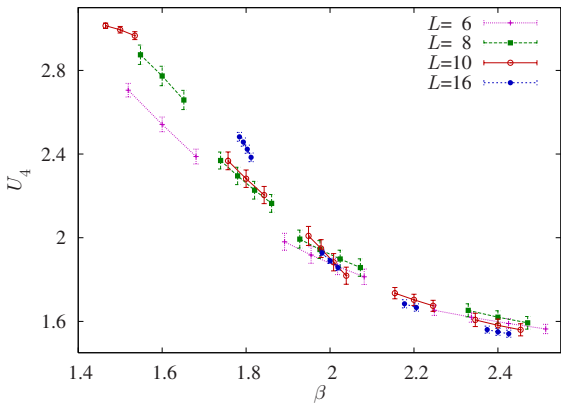

FIG. 3. (Color online) The cumulant U_4 as defined in Eq. (8) as a function of β for $d=3$ systems of different volumes.

in bin 0 in each sample, and averaging this quantity over the disorder. In other words, we define $\delta_n O \equiv \overline{\langle O\rangle_n - \langle O\rangle_0}$. This way, one can obtain much smaller statistical uncertainty: we plot this quantity for the nonconnected susceptibility in Fig. 1 by drawing the errors with thick lines.

For both β values of Fig. 1 both indicators show that convergence has been reached. Errors in $\delta_n \chi$ (thick error bars) are much smaller, but they still show that the last part of our samples has reached a steady state (even if the error is very small, all the data of the last bin are at the level of one standard deviation from zero: also notice that the data for different data bins are correlated, which implies that correlated discrepancies have to be expected). We can claim that the data of the $n=0$ bin are surely well thermalized, and we use them for computing the equilibrium expectation values that we discuss in this paper.

We have also estimated the integrated autocorrelation time τ for the observables that we have measured: we want to be sure that the total time length of our numerical simulation is far larger than τ.

In $d=3$, for our larger system $L=16$, at $\beta=2.4$ (a high value of β, deep inside the broken phase), we find that for the internal energy $\tau=5\times10^7$ EMCSs (and it turns out to be smaller for the other observables). This implies that our numerical simulation has been running for a time close to 12τ. In $d=4$, the length of the numerical simulation of the $L=16$ system at β values close to the critical point turns out to be close to 10τ.

We have also used a further test of thermalization by considering the data of the $n=0$ bin. We have done that by selecting a set of β values to use as starting points of the reweighting extrapolation.[38] Figures 2 and 3 show an example of how data originated from different disorder samples and independent numerical simulations yield consistent results. The choice of using a different set of samples for different β values (the starting points of the different reweightings that appear in the figure as neighboring groups of points of the same type) does not optimize the quality of the final extrapolation of the data (in the full β interval that we consider), but gives a further check of both the quality of the thermalization and of the quality of the sample average. In our case, the test is obviously successful.

Even if these general thermalization checks are very useful and they give strong hints that the system is thermalized, the Z_2 symmetry of the model (see Sec. II A), which has been introduced exactly with this goal in mind, is crucial to check thermalization. Let us repeat that the allowed couplings have been selected exactly such that the probability distribution of the modified overlap, $P(q)$, has to be symmetric at equilibrium. We show, in Figs. 4 and 5, $P(q)$ for $d=3$ and $d=4$ (computed by using the data of the $n=0$ bin—i.e., the last half of the data of the numerical simulation). These disorder-averaged distributions show very clearly the expected symmetry.

At last we have also studied the dynamics of different observables (for example of the modified overlap) in individual samples and we show an example in Fig. 6. We can observe a number of complete reversals of the global modified overlap, which gives us a new estimate of the time scale on which the system becomes modified: this time scale is compatible with what we have estimated before. We stress again that the determination of this time scale is further evidence that we are indeed at thermal equilibrium.

We believe that this discussion clearly shows that it is safe to use for an equilibrium analysis the data from the $n=0$ bin (i.e., the last half of the simulation), since it is fully thermalized.

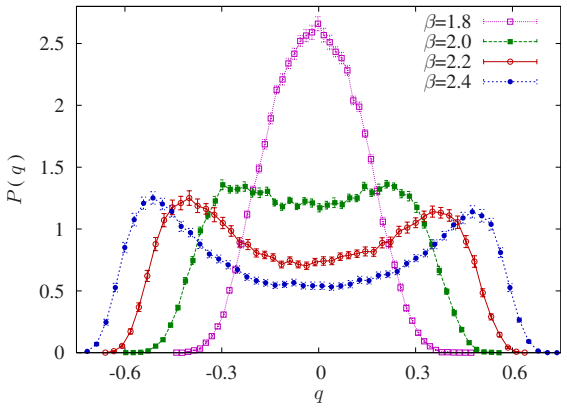

FIG. 4. (Color online) Distribution of the overlap in the $d=3$, $L=16$ system at several temperatures.

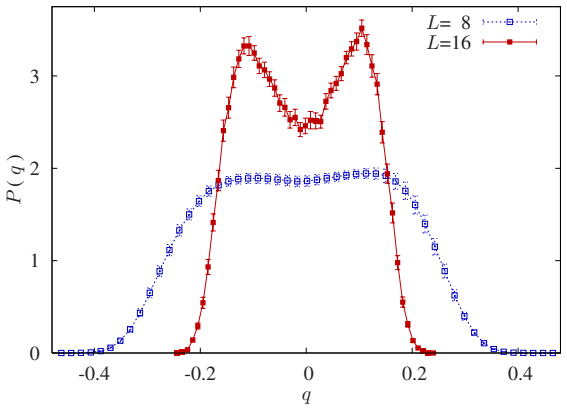

FIG. 5. (Color online) Distribution of the overlap in the $d=4$ model at low temperature ($\beta=1.44$) for two different lattice sizes.

IV. RESULTS FOR THE $d=3$ MODEL

We show in Fig. 2 the correlation length in units of L as a function of β for the three-dimensional (3D) model. In the high-temperature regime the curves for different lattice sizes are well separated: for increasing β the different curves approach each other, and for values of β close to 2.3 they seem to have merged in a single curve. In the limits of our statistical accuracy, we do not see any sign of a splitting of the curves in the high-T phase (a crossing point at T_c and a splitting in both the low-T and high-T phases is the usual signature of a usual phase transition): such a merging (without an eventual splitting) for increasing β is what would happen in a Kosterlitz-Thouless (KT) transition (see, for example, Ref. 42).

The first (of the many) delicate issue about this potential behavior concerns thermalization of the system: we have to be sure that we are not being misled by the fact that we have not thermalized the larger lattice sizes (this could produce an effect hiding a crossing in the high-β region). This is why we have studied, and discussed before, thermalization in detail: the thermalization checks described in Sec. III make us confident that we have reached equilibrium for all the lattice sizes that we have considered. We should not forget that

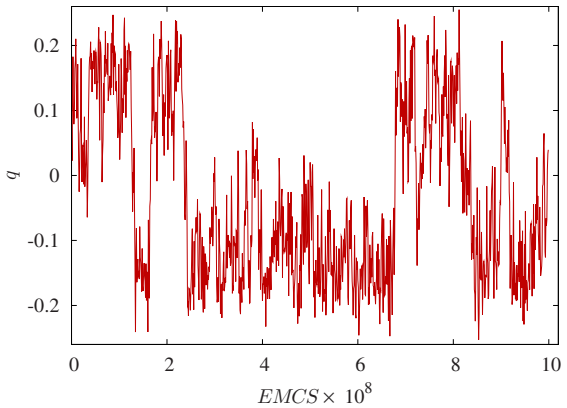

FIG. 6. (Color online) Evolution of the overlap of a representative sample of the $d=4$ model, $L=16$ system. Here $\beta=1.5$.

there are other possible issues that could hide from us, even in a very-large-scale simulation like the one discussed here, the asymptotic result: we could need, for example, a better statistical accuracy to discriminate a weak crossing, we could need large lattices to see the crossing appearing, or we could need to go to higher β values. The issue of a very weak transition is a very delicate one, and reliable statements must be phrased with great care. Here we claim that a KT scenario is a possible choice given the data that we have been able to measure in $d=3$,

In a KT scenario the quantity ξ/L is expected to remain invariant in a finite low-temperature region adjacent to the critical point. One way to be quantitative about that is to compute the crossing points $\beta_c^{L_1,L_2}$ for the dimensionless quantity U_4; see Eq. (11). In Fig. 3, we plot the cumulant U_4 for several lattice sizes. The curves for different lattice sizes cross close to $\beta=2.0$ (look, for example, at the $L=8$ and the $L=16$ lattices) at a temperature where the curves for ξ/L on different lattice sizes did not yet merge (i.e., where the correlation length has the high-T behavior). The region of the crossing is quite narrow, so that is very implausible that the scaling corrections to U_4 (usually larger than that of ξ/L) will shift the crossings as much as to get them close to $\beta=2.4$. Therefore, within our numerical accuracy, we do observe that ξ/L remains invariant in an interval of temperatures lower than that of the crossings of the cumulant.

The features we have described are consistent with a transition of the KT type.[42] Nevertheless, as we have discussed before, many possible effects could lead to difficult conclusions (for example, the value of the lower critical dimension to be slightly smaller than 3). It is clear, in any case, that in $d=3$ we are indeed sitting very close to the lower critical dimension.

V. RESULTS FOR THE $d=4$ MODEL

The authors of Ref. 6, where the CRPPG model that we investigate here was proposed, found that the four-dimensional CRPPG undergoes a transition to a spin-glass phase at $T\approx 1.5$ (by analyzing lattices of size $L=4$ and 5).

In order to analyze the transition, we study here the scaling behavior of quantities as ξ/L and U_4, that are expected to be L independent at the critical point. In Fig. 7 we plot the correlation length in units of the lattice size as a function of β. The reweighting extrapolations of these quantities for pairs of lattices L_1 and L_2 do intersect in the region around $\beta=1.41$. In order to be sure of the existence of the crossing we have thermalized lattices of linear size $L=8$ and $L=16$ deep in the low-temperature region: the normalized correlation length of the larger lattice is well above the one of the smaller lattice for β values ranging from 1.44 to 1.5.

In Fig. 8 we bring the region closer to our putative crossing. In this region we have also a thermalized lattice of linear size $L=12$, and we include the $L=12$ data in the figure and in our analysis.

In Table III we give the values of the crossing points $\beta_c^{L_1,L_2}$ obtained by the crossing of the ξ/L curves. Already from Fig. 8 it is clear that the accuracy of the size-dependent estimates $\beta_c^{L_1,L_2}$ is not high enough to allow an estimation of

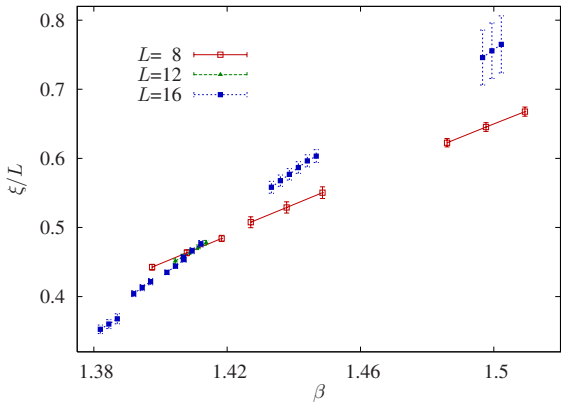

FIG. 7. (Color online) Correlation length in units of L as a function of β in the $d=4$ model.

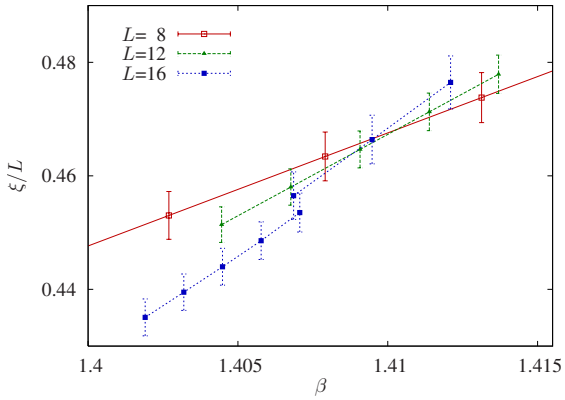

FIG. 8. (Color online) Close-up of the data of Fig. 7 close to the estimated critical point.

the scaling corrections. This is because reaching thermal equilibrium for $L>16$ was not in the scope of our numerical simulation (bound to run on a single FPGA chip), while lattices with linear size $L<8$ would have probably been too small to show the true asymptotic scaling corrections.

Since the cumulant U_4 scales like ξ/L at the critical point, it might have played the same role than ξ/L [by using Eq. (11)]. However, we find that it has much larger scaling corrections than ξ/L, and that these corrections shift the crossing points to higher temperatures, out of the range that we have analyzed (and where we believe the real asymptotic critical behavior can be observed). We have therefore not used U_4 in our study of the critical point. Our results compare fairly with the ones obtained in Ref. 6 by analyzing systems of linear sizes $L=4$ and $L=5$ (β must be renormalized since our Hamiltonian differs by a factor of 2 from the one of Ref. 6).

To obtain the critical exponents we consider the operators $\partial_\beta \xi$ and χ, whose associated exponents [see Eq. (10)] are $x_{\partial_\beta \xi}=\nu+1$ and $x_\chi=\gamma=\nu(2-\eta)$. Taking the logarithm of the quotients of these expectation values at the crossing points of ξ/L, we obtain the effective size-dependent exponents that we show in Table III. We can summarize our best estimate for the $d=4$ exponents as $\beta_c=1.41(1)$, $\xi^*/L=0.47(2)$, $\nu=1.1(2)$, $\eta=-0.31(3)$, and $\gamma=2.5(4)$: these errors are statistical in nature and cannot, obviously, fully take care of the systematic effects.

As was happening in the determination of the value of the critical coupling, the estimated exponents lack the precision necessary for obtaining a reliable infinite-volume extrapolation. Reference 6 quoted a value of γ in the range between 1.3 and 1.5, obtained from a study of the overlap susceptibility in the warm phase of a lattice $L=8$. Although our estimate is not very close to this value, it is clear that we are still dealing with lattice of intermediate size and that a careful analysis of scaling corrections, which we hope will soon be possible, will probably lead to a reconciliation of these results. Our results should characterize, if universality holds, the spin-glass transition to a Potts glass, independently from the detailed model one selects.

Finally, we also show in Table III the finite-size estimates of the universal quantity ξ^*/L—i.e., ξ/L evaluated at the critical coupling.

VI. CONCLUSIONS

We have presented a numerical study of the four-state CRPPG model in $d=4$ and $d=3$: we have used Monte Carlo simulations, reweighting techniques, and a finite-size scaling analysis. In $d=3$ our evidence clearly shows that we are very close to the lower critical dimension and suggests that a Kosterlitz-Thouless like behavior is possible, even if we could be dealing with a transient effect. In $d=4$ we are able to collect a large number of thermalized samples for systems defined on large lattices of linear size $L=16$. Because of such a large-scale numerical simulation, we are able to qualify the spin-glass transition first found in Ref. 6 and we obtain size-dependent estimates of the critical coupling of the critical exponents ν and η and of the scale-invariant quantity ξ^*/L.

In both cases, the use of a FPGA gives us the power needed to achieve thermalization, a target very ambitious for standard computers. We have been very careful in checking

TABLE III. Our best estimates for the size dependent effective critical coupling and for a number of universal quantities, as obtained from (L_1,L_2) pairs. γ is obtained from the hyperscaling relation $\gamma=\nu(2-\eta)$.

L_1	L_2	$\beta_{c,\xi/L}^{L_1,L_2}$	ξ^*/L	ν	η	γ
8	12	1.41(1)	0.47(2)	1.1(1)	−0.35(3)	2.6(2)
8	16	1.41(1)	0.47(1)	1.1(2)	−0.33(2)	2.5(4)
12	16	1.41(1)	0.46(2)	1.0(4)	−0.29(5)	2.4(9)

thermalization, and also as a result of the built-in symmetry of the CRPPG, we have succeeded in this task.

ACKNOWLEDGMENTS

Numerical computations have been performed at BIFI. We acknowledge partial financial support from CAM-UCM and UCM-BSCH, and from MEC through research contracts Nos. FIS2006-08533-C03 and TEC2007-64188. J.L.V. is supported by DGA. We thank Stefano Mossa, Giorgio Parisi, and Cristina Picus for a number of conversations about the glassy Potts models and more. We thank Raffaele Tripiccione and all the JANUS Collaboration for their continuous help, which could not have been more important for us.

APPENDIX: THE FPGA DEVICE

The problem of the glassy state, for example, is a typical problem of very high complexity. A large (maybe infinite) number of time scales is involved, and numerical simulations have to try to give hints about dynamics at very long times: very large correlation and thermalization times imply that, already on lattices of medium size, a huge computational effort is required. This is a typical situation where conventional computers could be not enough to do the job.

The use of FPGA programmable chips for the simulation of spin systems was proposed several years ago[43]: conventional computers are not optimized toward the computational tasks relevant for our typical calculation, and a FPGA can be programmed (at run time) in order to optimize the execution of the specific problem that one wants to solve.

FPGA devices come with numerous embedded and sizable memory blocks (RAM blocks) and thousands of configurable logic blocks with programmable interconnections. A configurable logic blocks can be programmed to perform complex logic operations and provide storage (flip-flop registers) at the same time.

A number of features that characterize our model are indeed optimal for being dealt with by a FPGA: we have discrete variables that can take a small number of values (4 for our $p=4$ system), and the interaction is local in physical space. The Metropolis algorithm and the random number generators discussed in Sec. III C have been implemented in the FPGA in a very effective way.

RAM blocks have a natural 2D (width $\times$ depth) grid structure. A 3D cubic matrix of bits can be obtained by *stacking* many of them, and access to all of them with the same memory address corresponds to addressing an entire plane in a 3D grid. We consider one such structure per each bit needed to represent fields (and interactions) defined on the sites of a simple cubic lattice.

Locality of interactions (nearest neighbors) allows for a high grade of internal parallelism: in a checkerboard scheme, all black or all white sites of a lattice plane can be updated simultaneously (i.e., at the same clock cycle). Moreover, when simulating two real replicas and mixing black (white) sites of a system with white (black) ones of its replica, all sites in a plane can be processed in parallel. Simultaneous local updates can then be performed by replicating small computation cells, each executing the few simple logical operations to compute local energies and including a 32-bit comparator for the Metropolis test. Precomputed transition probabilities (which allow to avoid lengthy computations of transcendental functions) are stored as several small look-up tables in configurable logic (*distributed* RAM) and addressed by the computed energy variations values (each look-up table serves two distinct computation cells). The iterative processes involving 32-bit integer arithmetics for random number generators have also been *parallelized* by cascading many 32-bit integer adders and XORs, and allowing for the generation of hundreds of 32-bit random numbers per clock cycle. For further details, see Ref. 32.

We use the FPGA device Virtex 4/LX200, manufactured by Xilinx. Depending on lattice size and number of parallel updates (between 64 and 256) our designs run at clock speeds between 50 and 100 MHz.

In Ref. 32 its performances have been compared with the ones of a 3.2-GHz Pentium IV device: for the $d=3$ model the FPGA performs 1800 times faster than a Pentium, while this factor is 2300 in $d=4$.

[1] E. Gardner, Nucl. Phys. B **257**, 747 (1985).
[2] D. Elderfield and D. Sherrington, J. Phys. C **16**, L497 (1983).
[3] D. Elderfield and D. Sherrington, J. Phys. C **16**, L971 (1983).
[4] D. J. Gross, I. Kanter, and H. Sompolinsky, Phys. Rev. Lett. **55**, 304 (1985).
[5] H. Nishimori and M. J. Stephen, Phys. Rev. B **27**, 5644 (1983).
[6] E. Marinari, S. Mossa, and G. Parisi, Phys. Rev. B **59**, 8401 (1999).
[7] S. Franz, M. Mézard, F. Ricci-Tersenghi, M. Weigt, and R. Zecchina, Europhys. Lett. **55**, 465 (2001).
[8] A. Cavagna, I. Giardina, and T. S. Grigera, Europhys. Lett. **61**, 74 (2003); A. Cavagna, I. Giardina, and T. S. Grigera, J. Chem. Phys. **118**, 6974 (2003).
[9] F. Krzakala and L. Zdeborová, EPL **81**, 57005 (2008).
[10] K. Binder and J. D. Reger, Adv. Phys. **41**, 547 (1992).
[11] See, e.g., M. Mézard, G. Parisi, and M. A. Virasoro, *Spin Glass Theory and Beyond* (World Scientific, Singapore, 1987).
[12] D. J. Gross and M. Mézard, Nucl. Phys. B **240**, 431 (1984).
[13] T. R. Kirkpatrick and P. G. Wolynes, Phys. Rev. B **36**, 8552 (1987).
[14] T. R. Kirkpatrick and D. Thirumalai, Phys. Rev. B **37**, 5342 (1988).
[15] W. Götze and L. Sjögren, Rep. Prog. Phys. **55**, 241 (1992).
[16] J. P. Bouchaud, L. F. Cugliandolo, J. Kurchan, and M. Mézard, in *Spin Glasses and Random Fields*, edited by A. P. Young (World Scientific, Singapore, 1997).
[17] K. Binder, in *Spin Glasses and Random Fields*, edited by A. P. Young (World Scientific, Singapore, 1997).
[18] J. R. Banavar and M. Cieplak, Phys. Rev. B **39**, 9633 (1989).
[19] J. R. Banavar and M. Cieplak, Phys. Rev. B **40**, 4613 (1989).

[20] M. Scheucher, J. D. Reger, K. Binder, and A. P. Young, Phys. Rev. B **42**, 6881 (1990).
[21] M. Scheucher and J. D. Reger, Phys. Rev. B **45**, 2499 (1992).
[22] M. Reuhl, P. Nielaba, and K. Binder, Eur. Phys. J. B **2**, 225 (1998).
[23] O. Carmesin and K. Binder, J. Phys. A **21**, 4053 (1988).
[24] R. R. P. Singh, Phys. Rev. B **43**, 6299 (1991).
[25] B. Lobe, W. Janke, and K. Binder, Eur. Phys. J. B **7**, 283 (1999).
[26] L. W. Lee, H. G. Katzgraber, and A. P. Young, Phys. Rev. B **74**, 104416 (2006).
[27] C. Brangian, W. Kob, and K. Binder, Europhys. Lett. **59**, 546 (2002).
[28] C. Brangian, W. Kob, and K. Binder, J. Phys. A **36**, 10847 (2003).
[29] M. P. Eastwood and P. G. Wolynes, Europhys. Lett. **60**, 587 (2002).
[30] G. Toulouse, Commun. Phys. (London) **2**, 115 (1977).
[31] D. M. Carlucci, Phys. Rev. B **60**, 9862 (1999).
[32] F. Belletti, M. Cotallo, A. Cruz, L. A. Fernández, A. Gordillo, A. Maiorano, F. Mantovani, E. Marinari, V. Martin-Mayor, A. Muñoz-Sudupe, D. Navarro, S. Perez-Gaviro, J. J. Ruiz-Lorenzo, S. F. Schifano, D. Sciretti, A. Tarancón, R. Tripiccione, and J. L. Velasco, Comput. Phys. Commun. **178**, 208 (2008).
[33] E. Marinari, G. Parisi, and J. J. Ruiz-Lorenzo, in *Spin Glasses and Random Fields*, edited by A. P. Young (World Scientific, Singapore, 1997).
[34] B. Cooper, B. Freedman, and D. Preston, Nucl. Phys. B **210**, 210 (1982).
[35] D. Amit and V. Martin-Mayor, *Field Theory, the Renormalization Group and Critical Phenomena*, 3rd ed. (World-Scientific, Singapore, 2005).
[36] M. Falcioni, E. Marinari, M. L. Paciello, G. Parisi, and B. Taglienti, Phys. Lett. **108B**, 331 (1982).
[37] A. M. Ferrenberg and R. H. Swendsen, Phys. Rev. Lett. **61**, 2635 (1988).
[38] H. G. Ballesteros, L. A. Fernández, V. Martin-Mayor, A. Muñoz-Sudupe, G. Parisi, and J. J. Ruiz-Lorenzo, Nucl. Phys. B **512**, 681 (1998).
[39] H. G. Ballesteros, L. A. Fernández, V. Martin-Mayor, and A. Muñoz Sudupe, Phys. Lett. B **378**, 207 (1996).
[40] H. G. Ballesteros, L. A. Fernández, V. Martin-Mayor, and A. Muñoz Sudupe, Nucl. Phys. B **483**, 707 (1997).
[41] G. Parisi and F. Rapuano, Phys. Lett. **157B**, 301 (1985).
[42] J. M. Kosterlitz and D. J. Thouless, J. Phys. C **6**, 1181 (1973).
[43] A. Cruz, J. Pech, A. Tarancón, P. Tellez, C. L. Ullod, and C. Ungil, Comput. Phys. Commun. **133**, 165 (2001).